NACA RM A50I14a

N-770

NACA

RESEARCH MEMORANDUM

INVESTIGATION OF THE DOWNWASH AND WAKE BEHIND A TRIANGULAR WING OF ASPECT RATIO 4 AT SUBSONIC AND SUPERSONIC MACH NUMBERS

By Harold J. Walker and Louis S. Stivers, Jr.

Ames Aeronautical Laboratory
Moffett Field, Calif.

NATIONAL ADVISORY COMMITTEE
FOR AERONAUTICS

WASHINGTON
December 12, 1950

NATIONAL ADVISORY COMMITTEE FOR AERONAUTICS

RESEARCH MEMORANDUM

INVESTIGATION OF THE DOWNWASH AND WAKE BEHIND A TRIANGULAR WING OF ASPECT RATIO 4 AT SUBSONIC AND SUPERSONIC MACH NUMBERS

By Harold J. Walker and Louis S. Stivers, Jr.

SUMMARY

The effects of Mach number in the ranges between 0.50 and 0.95 and between 1.09 and 1.29 on the characteristics of the downwash and on the location of the wake behind a triangular wing of aspect ratio 4 have been determined from semispan model tests.

The streamwise sections of the wing were symmetrical double wedges having a thickness–chord ratio of 0.08 with the maximum thickness at the midchord point. The downwash angles corresponding to angles of attack between -10° and $+10^\circ$ were measured at a distance of approximately 0.8 root–chord length downstream from the trailing edge, and at four spanwise stations between 25 and 75 percent of the wing semispan in each of two planes above the extended chord plane of the wing. The Reynolds number of the tests, based on the mean aerodynamic chord, ranged from 0.8 to 1.1 million. The results of the investigation are presented together with calculated characteristics.

In general, a change in Mach number produced only small changes in the downwash angle. An increase in Mach number was accompanied by a gradual decrease in the rate of change of downwash angle with lift coefficient at zero angle of attack.

Satisfactory agreement between the experimental and calculated downwash characteristics near zero angle of attack could be obtained at subsonic Mach numbers if the characteristics were referred to lift coefficient rather than angle of attack. A less favorable agreement, however, was found at supersonic Mach numbers.

The vertical location of the wake at a distance of 3.44 root–chord lengths downstream from the trailing edge of the wing was essentially unaffected by Mach number at a given lift coefficient. At subsonic Mach numbers as high as 0.86, the wake profiles were nearly symmetrical at the lower angles of attack; whereas at a Mach number of 1.29 the profiles

extended farther above the position of maximum total-pressure defect than below.

INTRODUCTION

The downwash behind lifting surfaces has been the subject of several experimental and theoretical investigations, which, in general, have been concerned with limited ranges of Mach number and types of plan form. For the range of Mach numbers corresponding to low-speed flow, a comprehensive study of the relationship between the downwash and the influence of the displacement and rolling up of the wake behind unswept wings of high aspect ratio is reported in reference 1. In this reference, it is shown for the configurations investigated that, in order to realize satisfactory agreement between experiment and theory, the displacement of the wake must be taken into account, but that the rolling up of the edges of the wake may be neglected. The effect of compressibility on the downwash at subcritical Mach numbers, as determined by the Prandtl-Glauert theory, is discussed in reference 2. In the supersonic range of Mach numbers, the downwash has been calculated in reference 3 for wings of several plan forms by means of the conical-flow method, and in references 4 and 5 for triangular wings through use of the concept of doublet distribution; but in neither method is the displacement and rolling up of the wake considered. From the experimental investigations of the downwash behind rectangular and triangular wings at a Mach number of 1.53 (references 6 and 7), it may be concluded that, for wings of low aspect ratio, the rolling up, as well as the displacement of the wake, must be considered in calculations of the downwash flow at moderate and high angles of attack. In reference 8, particular attention has been given to these properties of the wake for wings at subsonic and supersonic Mach numbers.

The present investigation was undertaken to ascertain experimentally the downwash characteristics and the location of the wake for a triangular wing at subsonic and low supersonic Mach numbers. The investigation should bridge, to some extent, the gap between the experimental investigations conducted at low subsonic Mach numbers and those conducted at supersonic Mach numbers. A limited number of comparisons between the present results and the corresponding characteristics calculated by the methods of references 1, 4, 5, and 8 are included to indicate the extent to which the measured characteristics can be predicted by theoretical methods.

SYMBOLS

c local wing-chord length

c_o wing root-chord length

C_L lift coefficient $\left(\frac{\text{lift}}{qS}\right)$

d downstream distance, measured from the quarter-chord point of the mean aerodynamic chord

M Mach number

q free-stream dynamic pressure

R Reynolds number based on mean aerodynamic chord

s wing semispan

S wing area

x,y,z Cartesian coordinates in the longitudinal, lateral, and vertical directions, respectively, with the origin at the apex of the leading edge of the wing and with the x axis lying along the intersection of the plane of the wing and the vertical plane of symmetry

α wing angle of attack, degrees

β $\sqrt{|1 - M^2|}$

δ_M jet-boundary correction factor for the downwash angle

ϵ downwash angle measured from the free-stream direction, degrees

APPARATUS

The tests were performed in the Ames 1- by 3-1/2-foot high-speed wind tunnel, which has a closed throat and is vented to the atmosphere in the settling chamber. The tunnel was equipped with a flexible throat which permitted operation at subsonic and supersonic Mach numbers.

The model consisted of a semispan triangular wing having a 45° semivertex angle (corresponding to an aspect ratio of 4), and was constructed of steel to the dimensions shown in figure 1. Sections of the wing in a streamwise direction were symmetrical double-wedge profiles having a thickness-chord ratio of 0.08 with the maximum thickness located at the midchord point. The wing surfaces were ground and polished, and the leading- and trailing-edge radii were approximately 0.002 inch.

A circular plate mounted flush with the tunnel wall, as shown in figure 2, served as a support for both the wing model and the apparatus for

measuring the downwash angles. The angle of attack of the model was varied by rotating the entire plate assembly.

The downwash angles were measured by means of the small probe shown in figure 1. The head of the probe was hemispherical in shape and contained two orifices located symmetrically with respect to the probe axis in a vertical plane through this axis. Total-pressure surveys of the wake from the model wing were made with a rake consisting of 50 tubes spaced at quarter-inch intervals. (See fig. 2.)

TESTS

Downwash angles were measured at the 25-, 50-, 62.5-, and 75-percent-semispan stations at distances between 0.8 and 0.9 root-chord length downstream from the trailing edge of the wing. The measurements at these locations were made at vertical distances of 0.20 and 0.40 root-chord lengths above the extended chord plane of the wing. (See fig. 1.) The investigation covered a range of angles of attack from -10° to $+10^\circ$ and a range of Mach numbers from 0.50 to 0.95 and from 1.09 to 1.29. The corresponding Reynolds numbers for these tests, based on the mean aerodynamic chord, varied from 0.85×10^6 to 1.10×10^6 as shown in figure 3. Downwash angle measurements could not be made at certain of the highest positive angles of attack because of the influence of the wake on the pressures indicated by the probe. At the highest subsonic Mach numbers, the highest angle attainable in the negative range was that at which the flow in the tunnel became choked.

Wake profiles at the 50-percent-semispan station were investigated at a distance of 3.44 root-chord lengths downstream from the trailing edge. The investigation covered a range of angles of attack from 0° to 10° at Mach numbers of 0.50, 0.70, 0.80, 0.86, and 1.29.

CORRECTIONS TO DATA

Stream-angle surveys with the model removed from the tunnel were made in a vertical plane at each spanwise station for the Mach numbers of this investigation. The measured stream angles were generally less than 0.3° and were applied as corrections to the measured downwash angles behind the wing.

For the subsonic range of Mach numbers, the angles of attack were corrected for the effects of the tunnel walls by the method of reference 9. The correction, which is shown in reference 10 to be independent of Mach number, is given by the expression

$$\Delta\alpha = 0.341\, C_L$$

[redacted]

The corresponding correction for the measured downwash angles, as calculated by the method of reference 11, is given by the expression

$$\Delta\epsilon = 1.493\ \delta_M\ C_L$$

where the factor δ_M is dependent upon the location of the point at which the downwash angle is measured. The variation of δ_M was found to be small over the ranges of spanwise and vertical locations at which the measurements were made. Hence, the values of δ_M used to determine the downwash-angle corrections were simply calculated for points along the line of intersection of the horizontal and vertical planes of symmetry of the wing (at zero angle of attack). These values, which are shown in figure 4, correspond to an elliptic spanwise loading on a 5-inch-semispan unswept lifting line located in the center of the 3-1/2-foot dimension of the tunnel, and include the effects of compressibility based on the relations for linearized compressible flow.

For the supersonic range of Mach numbers, the downwash angles and the location and thickness of the wake were measured at positions which were essentially devoid of abrupt changes in pressure due to shock waves. Accordingly, the measurements made with the probe and the wake-survey rake are believed to be reliable.

The displacement thickness of the boundary layer on the tunnel wall at the position of the model was found to be approximately 0.12 inch within the Mach number range of the investigation. Some drainage of the low-energy air from the boundary layer of the wind tunnel into the regions of low induced pressure on the surface of the wing may have taken place in the course of tests; however, no attempt was made to assess the effects of this possible drainage.

RESULTS AND DISCUSSION

Downwash Characteristics

Variation of downwash angle with angle of attack.- In figures 5 and 6, respectively, the variation of downwash angle with angle of attack for the two vertical locations, 0.20 and 0.40 root-chord lengths above the extended chord plane of the wing, are presented for the range of Mach numbers and spanwise locations investigated. These data show that, in general, an increase in angle of attack is accompanied by a gradual increase in the slope of the curves. (See especially fig. 6.) This increase in slope is due to the fact that the points at which the downwash was measured were located above the trailing vortex sheet (or wake), and that the distance between these points and the vortex sheet

[redacted]

decreased as the angle of attack was increased. This effect of the displacement of the vortex sheet has been calculated in references 1 and 7.

For reasons which are not completely understood, some of the curves for the supersonic Mach numbers do not pass through the origins of the plots.

Rate of change of downwash angle with angle of attack.— The effect of Mach number on the rate of change of downwash angle with angle of attack at zero angle of attack (i.e., $(d\epsilon/d\alpha)_{\alpha=0}$) is shown in figure 7. Calculated values of $(d\epsilon/d\alpha)_{\alpha=0}$ are also shown in this figure, and curves based on these values are included in figures 5(a) and 6(a).

Since previous calculations have shown the spanwise variation of the downwash flow near the vertical plane of symmetry to be small, the calculated values in the present case, which were determined for the vertical plane of symmetry, are believed to be comparable with the experimental downwash angles at the 25-percent-semispan station. For the subsonic Mach numbers, the calculated values of $(d\epsilon/d\alpha)_{\alpha=0}$ were determined by the method of reference 1, using five U-shaped vortices to approximate an elliptic spanwise loading on the wing. The lifting lines of the vortices were located so as to pass through the quarter-chord point of the mean aerodynamic chord. The relations for linearized compressible flow were included in the calculations to determine the effect of compressibility. For the supersonic Mach numbers, calculated values of $(d\epsilon/d\alpha)_{\alpha=0}$ were obtained from reference 5, in which a lifting-surface theory is used to determine the downwash behind a flat triangular wing. Because the comparisons between experiment and theory are to be limited to small angles of attack, the effects of the displacement and rolling up of the vortex sheet are neglected in all these calculations.

In figures 5, 6, and 7, good agreement between experiment and theory is indicated at the lower Mach numbers. In figure 7 it is observed that, except at the highest subsonic Mach numbers, the effect of Mach number on the experimental values of $(d\epsilon/d\alpha)_{\alpha=0}$ is not significant. A similar trend is noted in figure 8 with regard to the experimental lift-curve slope, which was determined for the same wing in the investigation of reference 12.

Although the variations with Mach number of the experimental values of $(d\epsilon/d\alpha)_{\alpha=0}$ for the 25-percent-semispan station, shown in figure 7, are somewhat similar to those shown for the calculated slopes in the plane of symmetry, the differences between the magnitudes of the respective slopes are somewhat greater than those which may be attributed to the difference in spanwise location. This is particularly evident at the higher subsonic and at the supersonic Mach numbers. Since the downwash is more directly related to the lift coefficient than to the angle

of attack of the wing, it would be expected that any difference between the experimental and calculated values of $(dC_L/d\alpha)_{\alpha=0}$ would produce corresponding differences between the experimental and calculated values of $(d\epsilon/d\alpha)_{\alpha=0}$. Accordingly, experimental and calculated values of $(d\epsilon/dC_L)_{\alpha=0}$ were determined and are presented as a function of Mach number in figure 9. In the subsonic Mach number range, the results from experiment and theory now compare quite favorably, but in the supersonic range the experimental values appear to be higher than those predicted by theory. The higher experimental values for the supersonic Mach numbers are believed to have resulted from a greater loading near the vertical plane of symmetry of the wing than that predicted theoretically (elliptic loading).

It is indicated in figure 7 that the slope $(d\epsilon/d\alpha)_{\alpha=0}$ decreases with distance from both the wake center and the vertical plane of symmetry of the wing. The experimentally determined spanwise variation of $(d\epsilon/d\alpha)_{\alpha=0}$ is shown in figure 10. These results, in the supersonic Mach number range, are in qualitative agreement with the experimental and calculated results reported in reference 7 for a triangular wing of aspect ratio 2 and a Mach number of 1.53.

Wake Characteristics

Partial sketches of the wake profiles at the 50-percent-semispan location at a distance of 3.44 root-chord lengths downstream from the trailing edge of the wing are presented in figure 11. The locations of the positions of maximum total-pressure defect and of the boundaries of the wake with respect to the extended chord plane of the wing are shown for angles of attack ranging from 0° to 10.5° and for Mach numbers of 0.50, 0.70, 0.80, 0.86, and 1.29.

From figure 11, three significant observations may be made:

1. For each Mach number, an increase in angle of attack is accompanied by an upward displacement of the wake above the extended chord plane of the wing, and by an increase in the thickness of the wake.

2. For each angle of attack, an increase in Mach number gives rise, for the most part, to some thickening of the wake, but to little or no change in the location of the wake.

3. The wake profiles at the highest angles of attack differ markedly from those at the lower angles, and the profiles at the supersonic Mach number deviate to a considerable extent from those at the subsonic Mach numbers.

[redacted]

An examination of the profiles in detail is facilitated by grouping them into the types I, II, and III illustrated in figure 12. The type I profile, which is approximately symmetrical about the position of maximum total-pressure defect, corresponds to that generally observed at low angles of attack and at subcritical Mach numbers. Accordingly, no further discussion of this type is required.

Type II is representative of the profile that existed at the highest angles of attack (about 10°) in the subsonic Mach number range of the present investigation. This type has a very pronounced maximum total-pressure defect, denoted by A in figure 12, situated directly above a rather weak local maximum defect, denoted by B. It was reasoned that at these angles the trailing vortex sheet from the wing had rolled up to such an extent that the tip-vortex core appeared in the plane of the survey rake. The larger maximum defect (A) then corresponds to the rolled-up portion of the wake (tip-vortex core) and the smaller maximum defect (B), to the unrolled portion (vortex sheet), as illustrated in figure 13. An inboard movement of the tip vortex core to the vicinity of 50-percent-semispan station would be greater than that predicted for the case in which the spanwise loading is assumed to be elliptical. As has been shown in reference 8, such an inboard shift may result from an increase in the portion of the load carried near the vertical plane of symmetry. Although the spanwise loading for the wing of the present investigation was not known, an inboard shift of the loading for triangular wings has been observed in the experimental investigation reported in reference 13.

The type III profile, which is characterized by a more extensive region of large total-pressure defect (denoted by C, fig. 12) above the position of maximum defect, existed only at the supersonic Mach number, 1.29, at positive angles of attack. The greater defect in the upper portion of the profile at this Mach number possibly may be attributed to the combined effects of boundary-layer separation and shock waves originating on the wing. (See reference 14.) The profile for the angle of attack of 10.2° at Mach number 1.29 is believed to be a combination of types II and III. The maximum defect in this case probably corresponds to the rolled-up portion of the wake. The defect corresponding to the unrolled portion is not discernible.

The variation of the wake location with lift coefficient at the various Mach numbers is shown in figure 14. At lift coefficients near 0.55 (approximately 10° angle of attack), two groups of points are shown which correspond to the centers of parts A and B of the type II profile shown in figure 12. Calculated vertical locations of the vortex sheet at the 50-percent-semispan station of the wing and of the center of the tip-vortex core, determined from references 8 and 15, also are included in figure 14. These calculations are presented in order to indicate the

extent to which the location of the wake may be predicted, and to verify the previously assumed correspondence between the component parts of the type II profile and the rolled-up and unrolled portions of the wake. The location of the wake above the extended chord plane of the wing is dependent upon both the angle of attack and the lift coefficient, and, for linear lift curves, may be expressed in terms of the lift-curve slope. In order to eliminate any uncertainty in the correspondence between the experimental and calculated wake locations which could be attributed to the known difference between the experimental and calculated lift-curve slopes, the experimental slopes were used. The experimental lift-curve slope varies with Mach number as shown in figure 8; but, rather than present the wake locations for particular Mach numbers, regions are given, the boundaries of which were determined from the maximum and minimum values of the slope (which occur at Mach numbers of 0.92 and 1.29, respectively).

It may be seen in figure 14 that the experimental variation with lift coefficient of the vertical location of the wake above the extended chord plane of the wing is nearly linear, and is essentially independent of Mach number. The experimental points generally fall within the calculated regions, and the agreement is considered to be very good.

CONCLUDING REMARKS

It can be concluded from the foregoing investigation that no pronounced changes in the downwash angles at points behind a triangular wing of aspect ratio 4 occurred in the ranges of Mach numbers between 0.50 and 0.95 and between 1.09 and 1.29. An increase in Mach number within these ranges was accompanied by a gradual decrease in the rate of change of downwash angle with lift coefficient at zero angle of attack. At any particular Mach number, the downwash angle for a given angle of attack decreased with distance from the wake and/or the vertical plane of symmetry of the complete wing.

If based on lift coefficient rather than angle of attack, the calculated and experimental downwash characteristics at the subsonic Mach numbers were generally in good agreement. At supersonic Mach numbers less satisfactory agreement was obtained whether the characteristics were based on lift coefficient or angle of attack.

For a given lift coefficient, an increase in Mach number within the afore-mentioned ranges produced little or no change in the location of the wake at the 50-percent-semispan station at a distance of 3.44 root-chord lengths downstream from the trailing edge. The displacement of the wake above the extended chord plane of the wing increased with an increase in lift coefficient. The edges of the wake appeared to have

[redacted]

rolled inboard to the 50-percent-semispan station at angles of attack near 10°. At Mach numbers as high as 0.86, the wake profiles were essentially symmetrical at the lower angles of attack. At a Mach number of 1.29 the profiles extended farther above the position of maximum total-pressure defect than below. The correspondence between the experimental and calculated vertical locations of the wake and tip-vortex core above the extended chord plane of the wing was found to be good.

Ames Aeronautical Laboratory,
National Advisory Committee for Aeronautics,
Moffett Field, Calif.

[redacted]

REFERENCES

1. Silverstein, Abe, Katzoff, S., and Bullivant, W. Kenneth: Downwash and Wake Behind Plain and Flapped Airfoils. NACA Rep. 651, 1939.

2. Nielsen, Jack N., and Sweberg, Harold H.: Note on Compressibility Effects on Downwash at the Tail at Subcritical Speeds. NACA CB L5C09, 1945.

3. Lagerstrom, P.A., and Graham, Martha E.: Downwash and Sidewash Induced by Three-Dimensional Lifting Wings in Supersonic Flow. Douglas Aircraft Co., Inc., Rep. SM-13007, Apr. 1947.

4. Heaslet, Max. A., and Lomax, Harvard: The Calculation of Downwash Behind Supersonic Wings With an Application to Triangular Plan Forms. NACA TN 1620, 1948.

5. Lomax, Harvard, and Sluder, Loma: Downwash in the Vertical and Horizontal Planes of Symmetry Behind a Triangular Wing in Supersonic Flow. NACA TN 1803, 1949.

6. Perkins, Edward W., and Canning, Thomas N.: Investigation of Downwash and Wake Characteristics at a Mach Number of 1.53. I – Rectangular Wing. NACA RM A8L16, 1949.

7. Perkins, Edward W., and Canning, Thomas N.: Investigation of Downwash and Wake Characteristics at a Mach Number of 1.53. II – Triangular Wing. NACA RM A9D20, 1949.

8. Spreiter, John R., and Sacks, Alvin H.: The Rolling Up of the Trailing Vortex Sheet and Its Effect on the Downwash Behind Wings. Institute of Aeronautical Sciences Preprint No. 250, January, 1950.

9. Glauert, H.: Wind Tunnel Interference on Wings, Bodies, and Airscrews. British R. & M. No. 1566, Sept. 1933.

10. Goldstein, S., and Young, A. D.: The Linear Perturbation Theory of Compressible Flow With Applications to Wind Tunnel Interference. British R. & M. No. 1909, July, 1943.

11. Swanson, Robert S., and Schuldenfrei, Marvin J.: Jet-Boundary Corrections to the Downwash Behind Powered Models in Rectangular Wind Tunnels with Numerical Values for 7- by 10-Foot Closed Wind Tunnels. NACA ARR, Aug. 1942.

12. Stivers, Louis S., Jr., and Malick, Alexander, W.: Wind-Tunnel Investigation at Mach Numbers from 0.50 to 1.29 for an

[redacted]

All-Movable Triangular Wing of Aspect Ratio 4 Alone and with a Body. NACA RM A9L01, 1950.

13. Anderson, Adrien E.: Chordwise and Spanwise Loadings Measured at Low Speed on Large Triangular Wings. NACA RM A9B17, 1949.

14. Love, Eugene S.: Investigations at Supersonic Speeds of 22 Triangular Wings Representing Two Airfoil Sections for Each of 11 Apex Angles. NACA RM L9D07, 1949.

15. Westwater, F. L.: The Rolling Up of the Surface of Discontinuity Behind an Aerofoil of Finite Span. R. & M. 1692, British A.R.C., 1935.

[redacted]

y
0.25 s
0.50 s
0.625 s
0.75 s

x	z
1.86 c_o	0.20 c_o
1.81 c_o	0.40 c_o

Dimensions given in inches

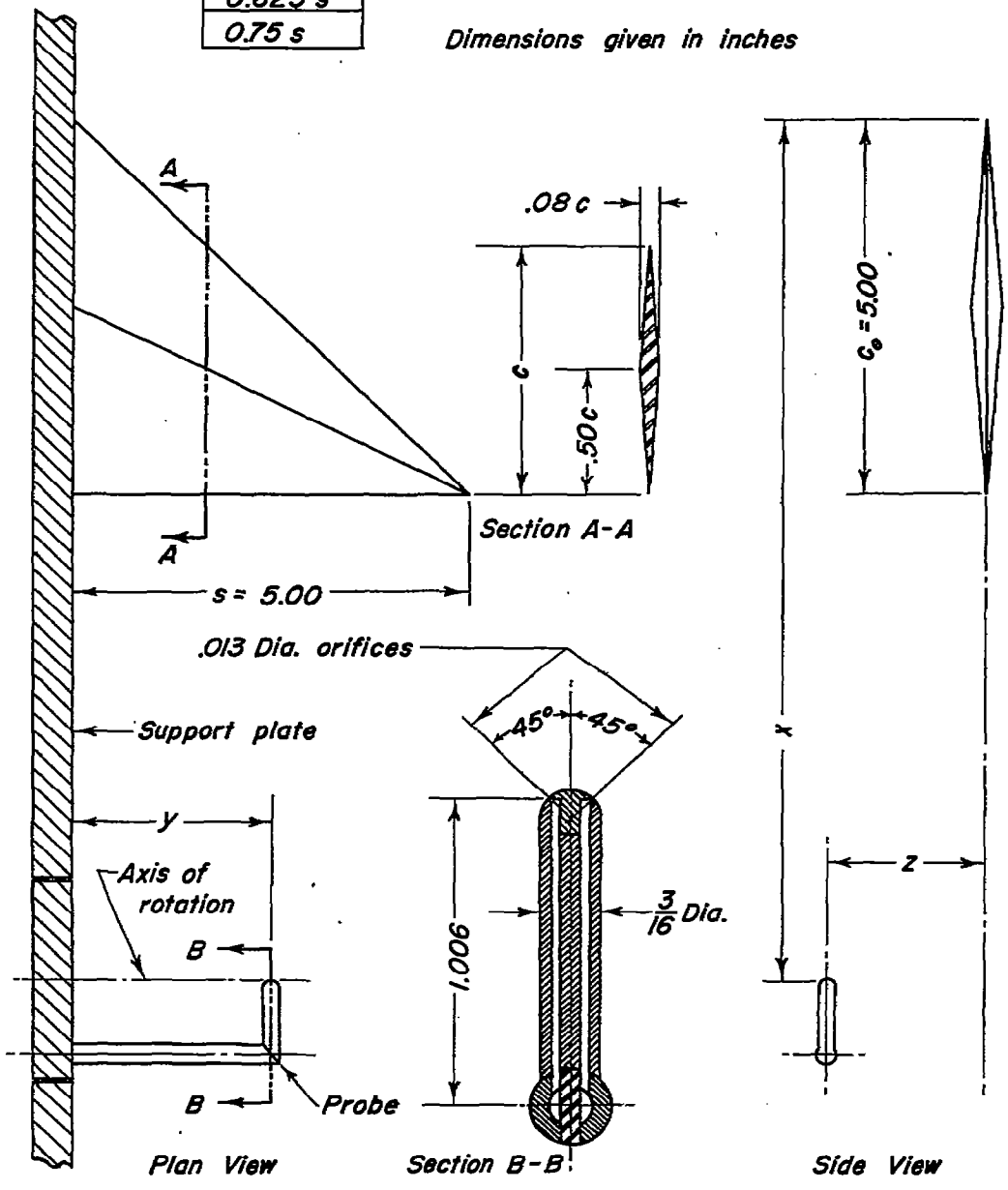

Figure 1.- Sketch of model and downwash probe, showing locations of downwash survey stations.

[redacted]

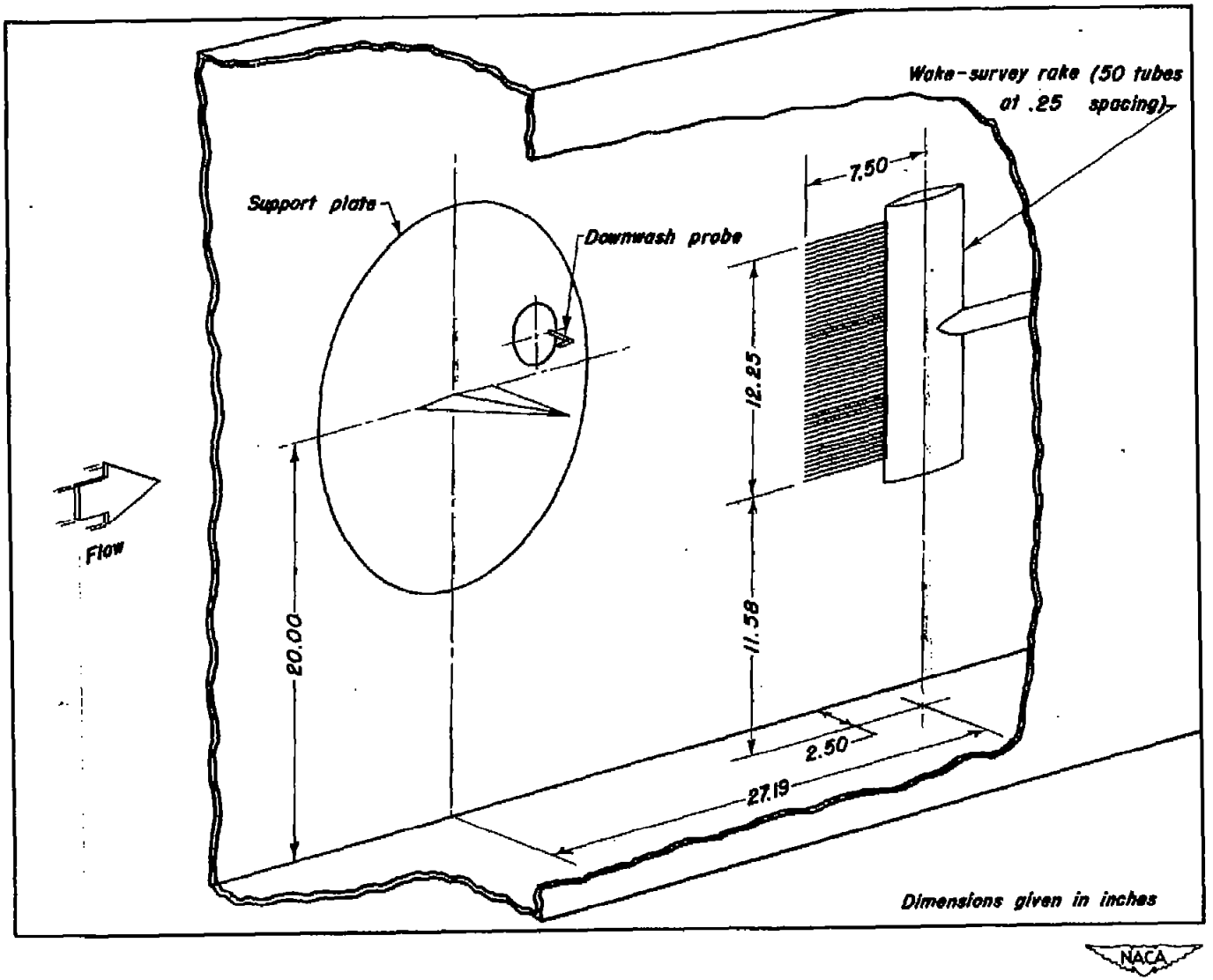

Figure 2. – Sketch of model support showing location of wake-survey rake.

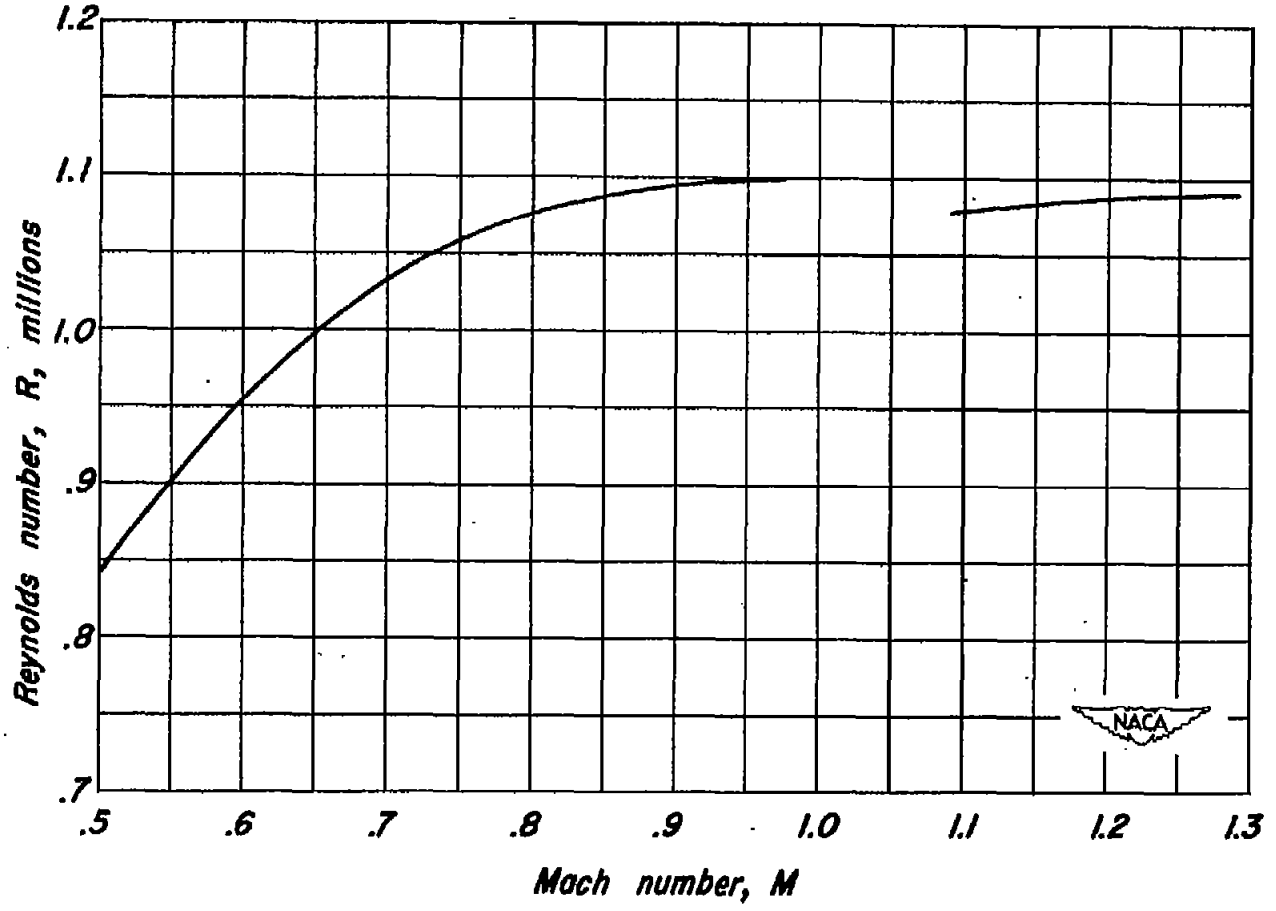

Figure 3. – Variation of Reynolds number with Mach number.

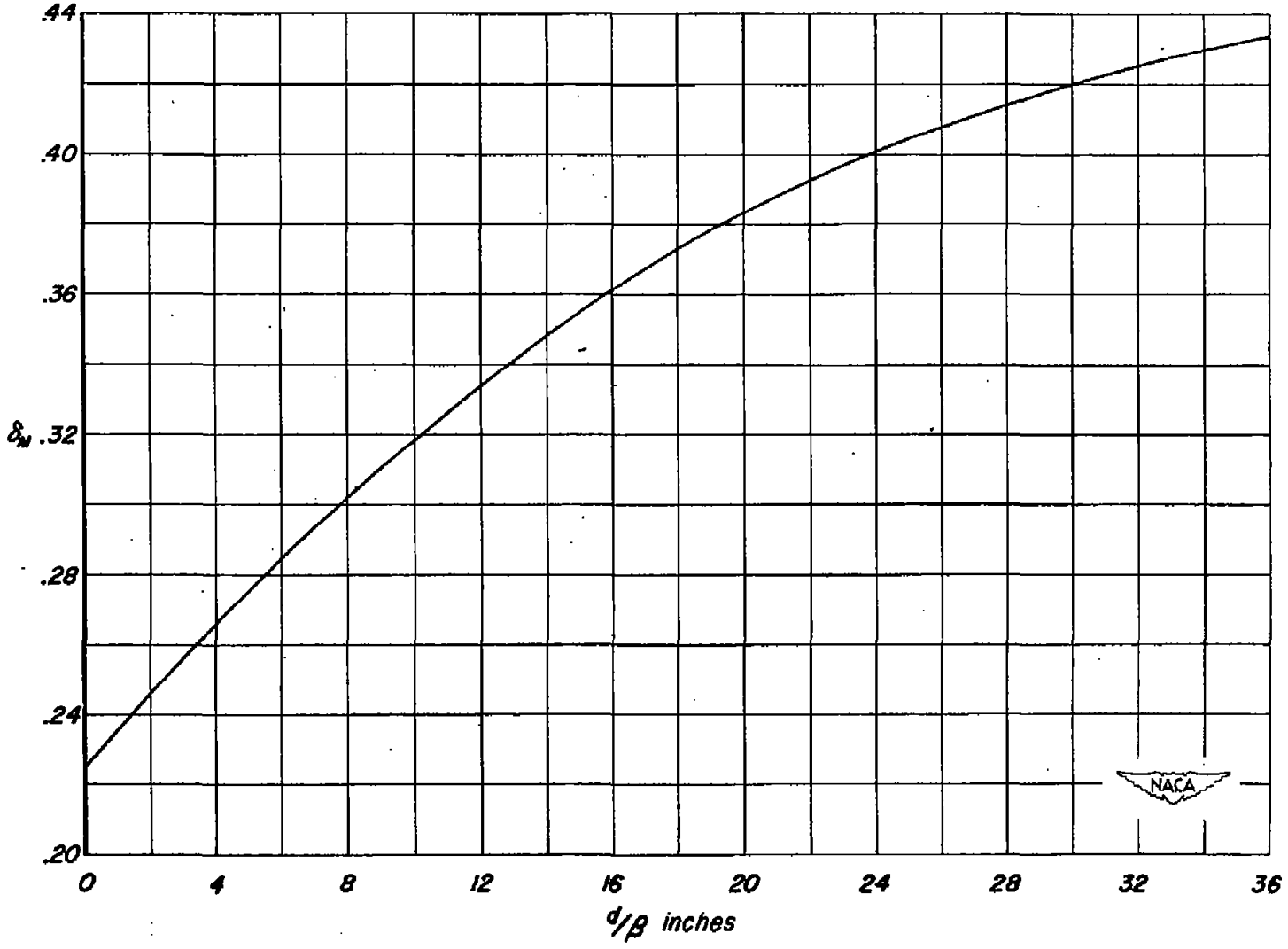

Figure 4. - Variation with distance (d/β) of the factor δ_M calculated for a 5-inch-semispan lifting line located in the center of the $3\frac{1}{2}$-foot dimension of a 1- by $3\frac{1}{2}$-foot wind tunnel.

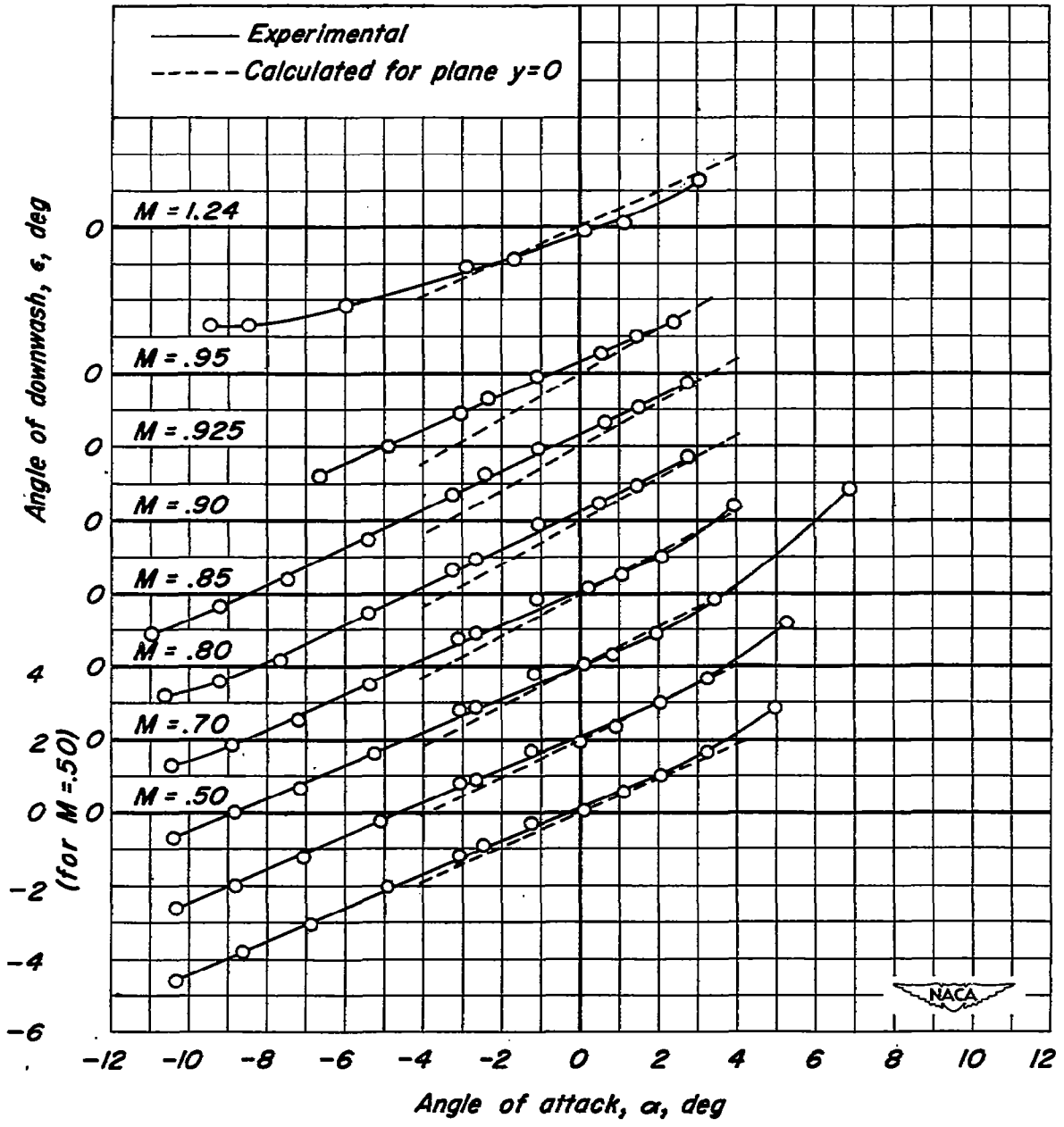

(a) y=0.25 s.

Figure 5.- Variation of angle of downwash with angle of attack at several Mach numbers ; x, 1.86 c_o and z, 0.20 c_o.

[redacted]

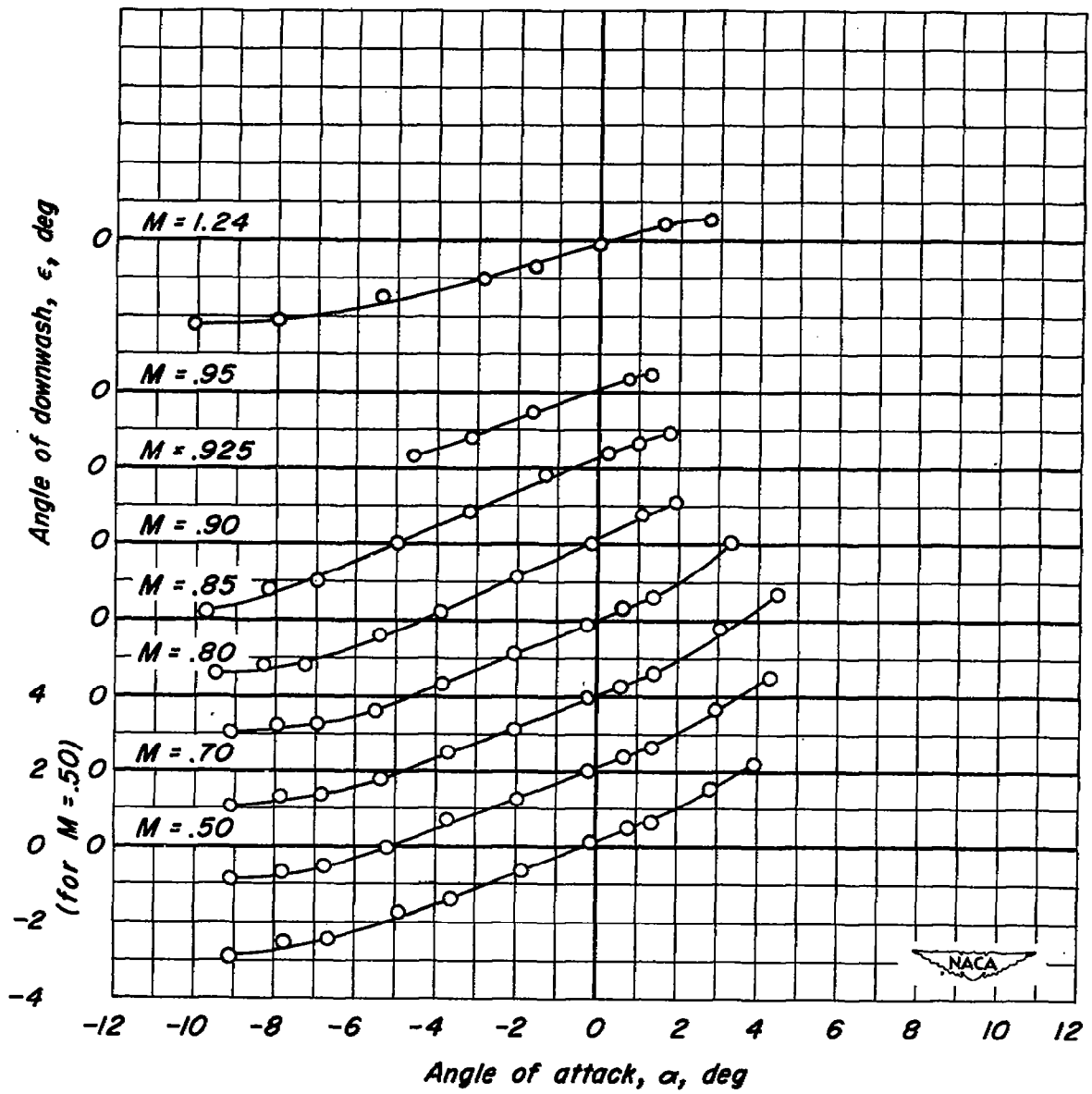

(b) y = 0.50 s .

Figure 5. - Continued.

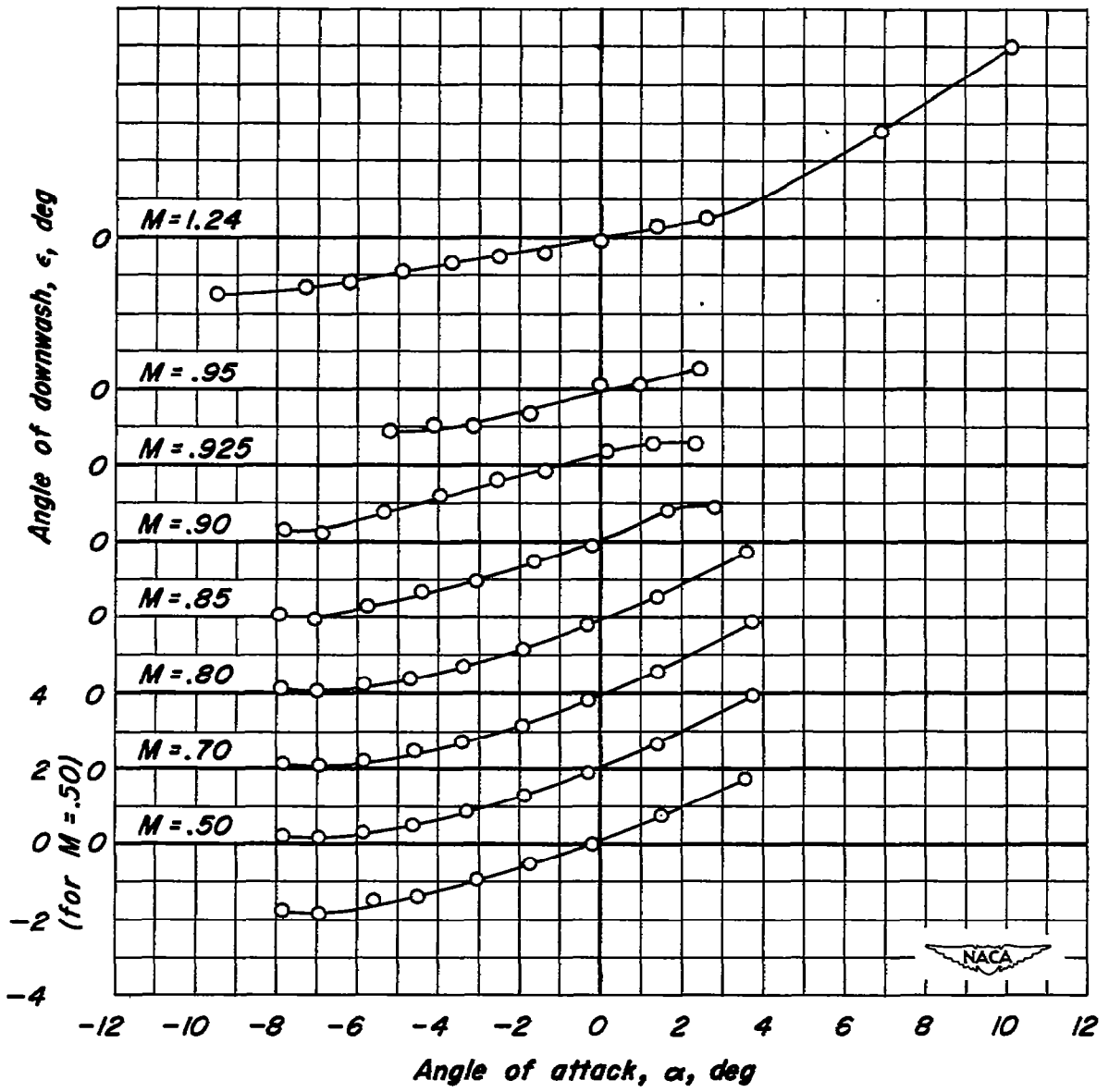

(c) y = 0.625 s.

Figure 5. - Continued.

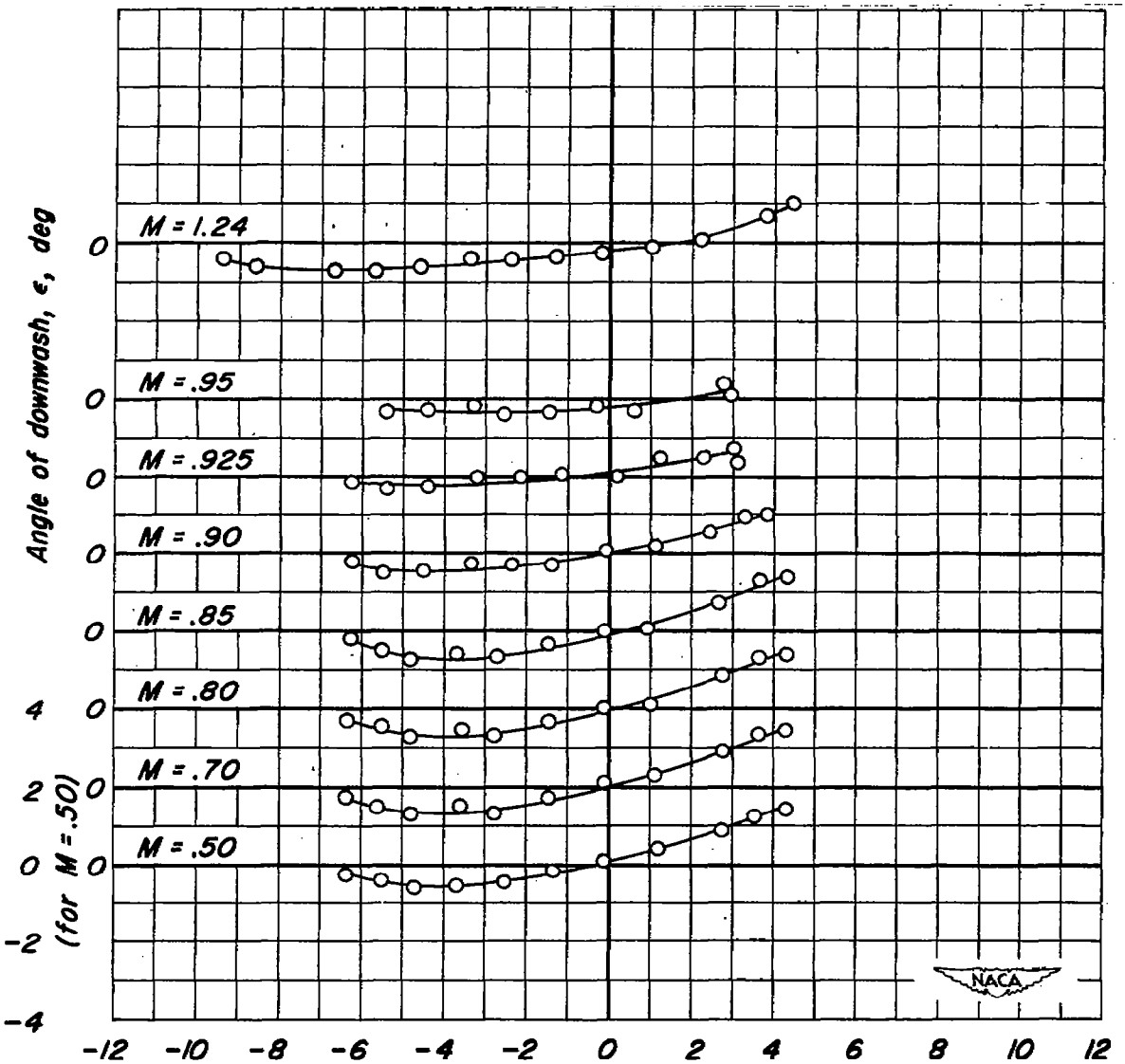

(d) $y = 0.75\,s$.

Figure 5. - Concluded.

[redacted]

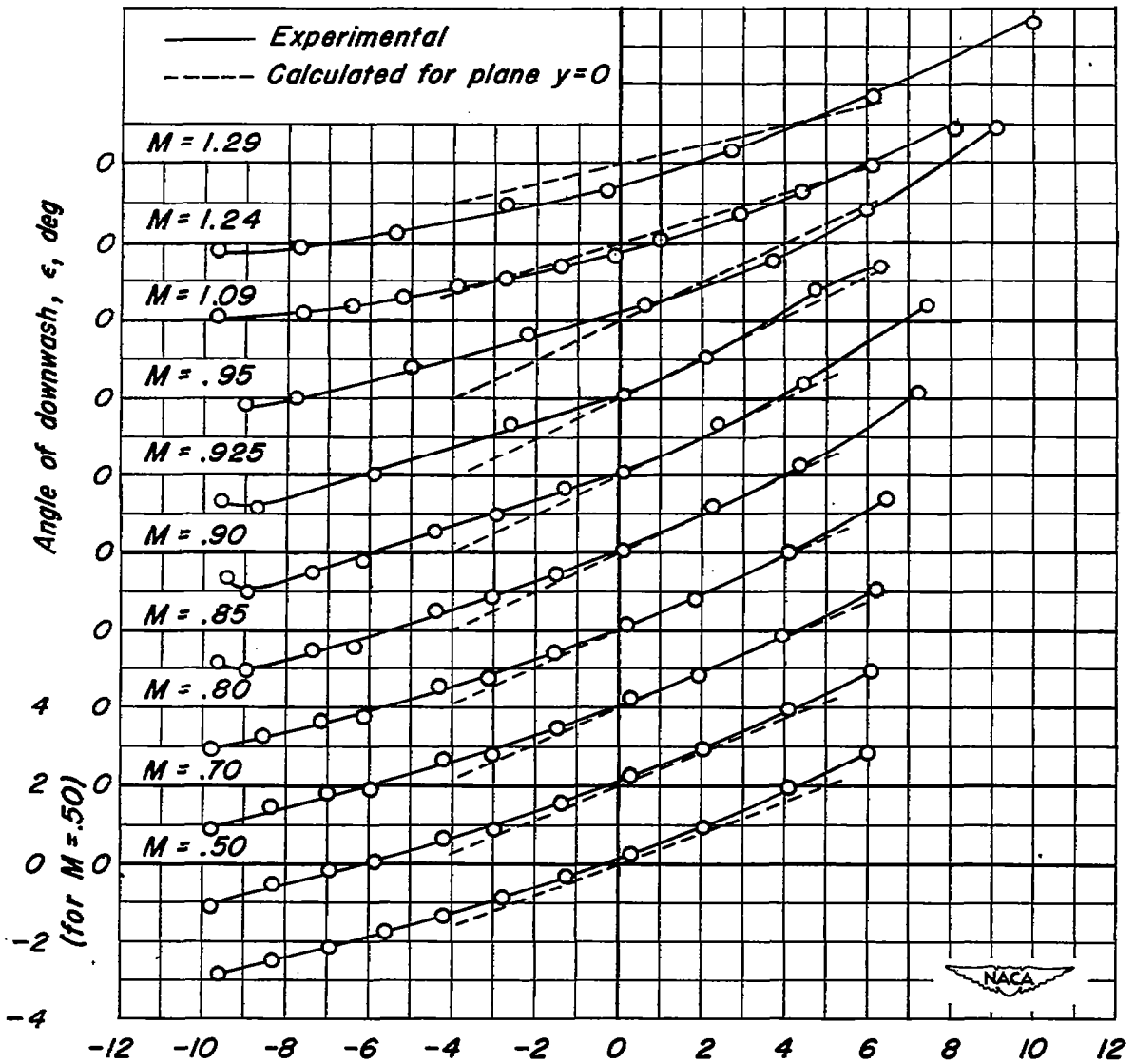

(a) $y = 0.25\ s$.

Figure 6.- Variation of angle of downwash with angle of attack at several Mach numbers; x, 1.81 c_o and z, 0.40 c_o.

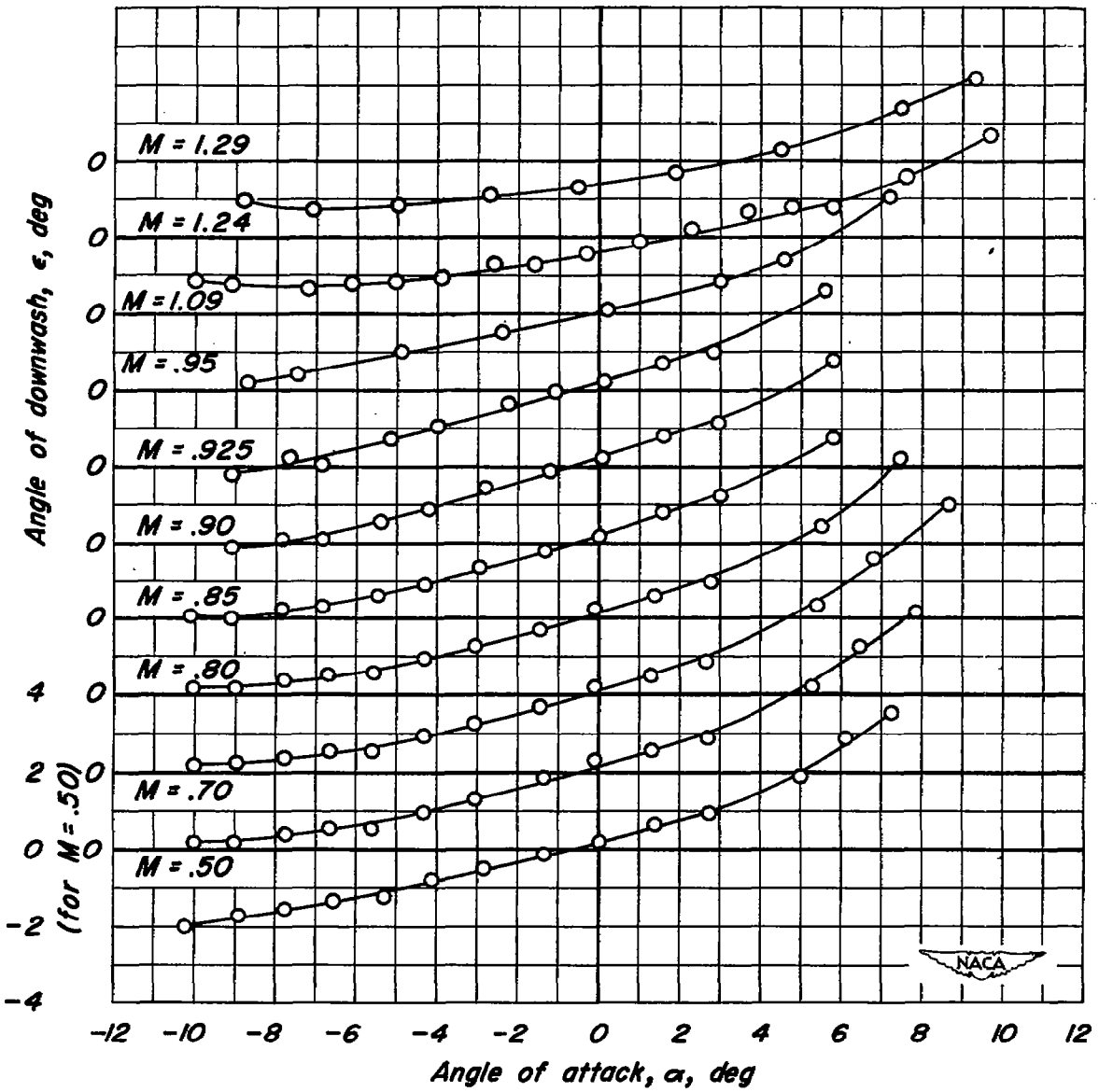

(b) y=0.50 s.

Figure 6. - Continued.

[redacted]

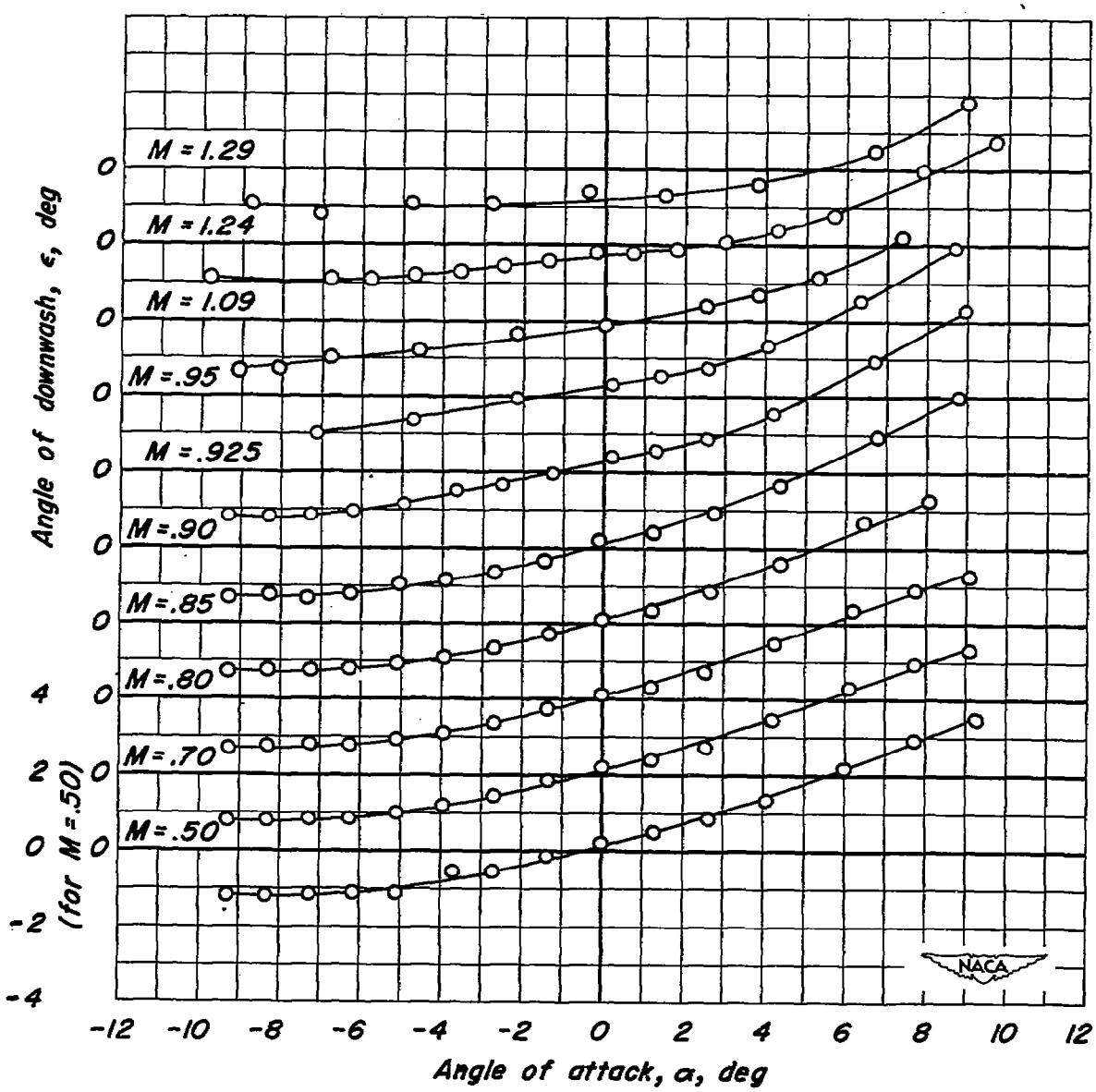

(c) $y = 0.625\ s$.

Figure 6. - Continued.

[redacted]

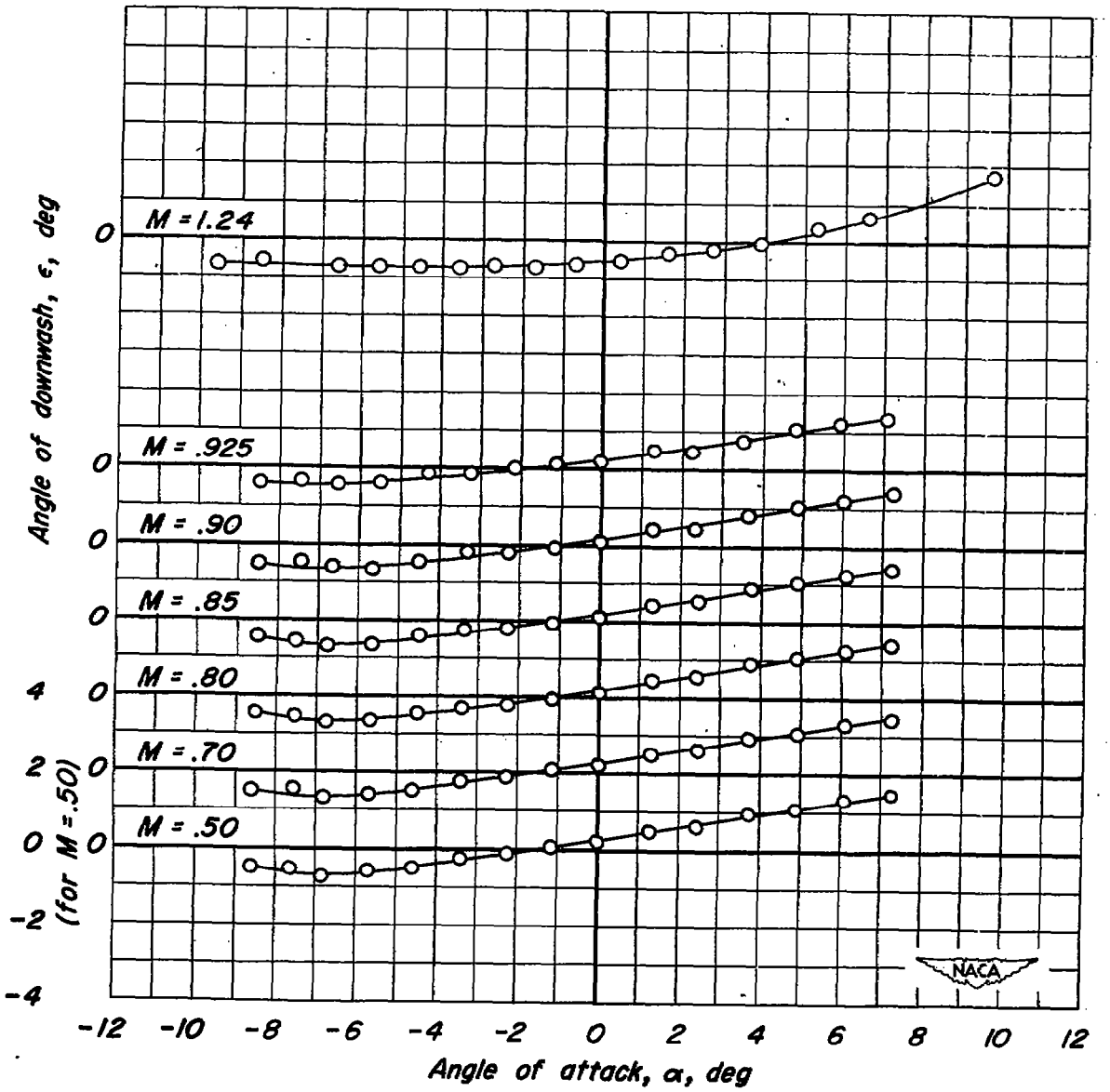

(d) $y = 0.75\ s$.

Figure 6. - Concluded.

[redacted]

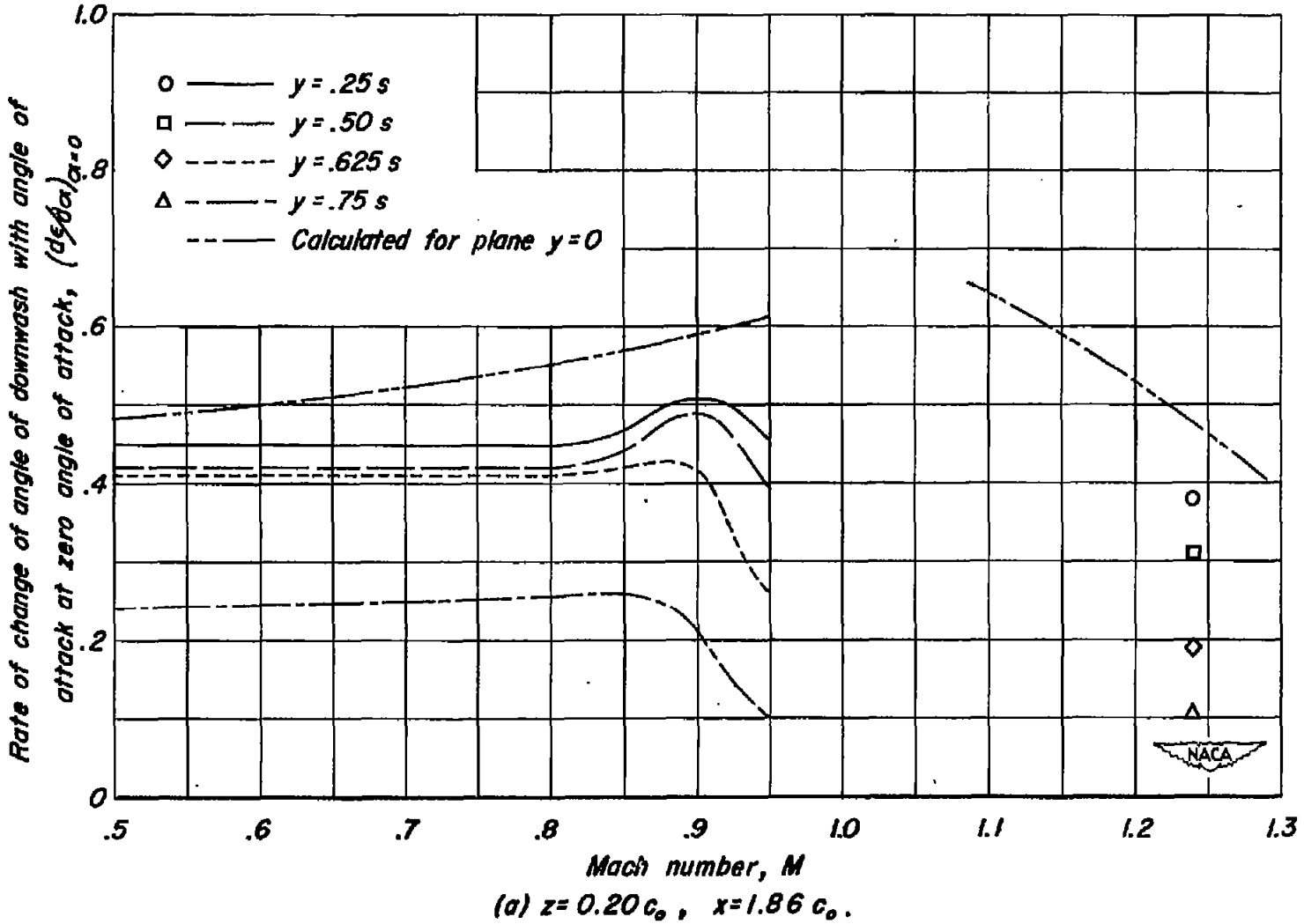

(a) $z = 0.20 c_o$, $x = 1.86 c_o$.

Figure 7. – Variation with Mach number of rate of change of angle of downwash with angle of attack at zero angle of attack for several spanwise stations.

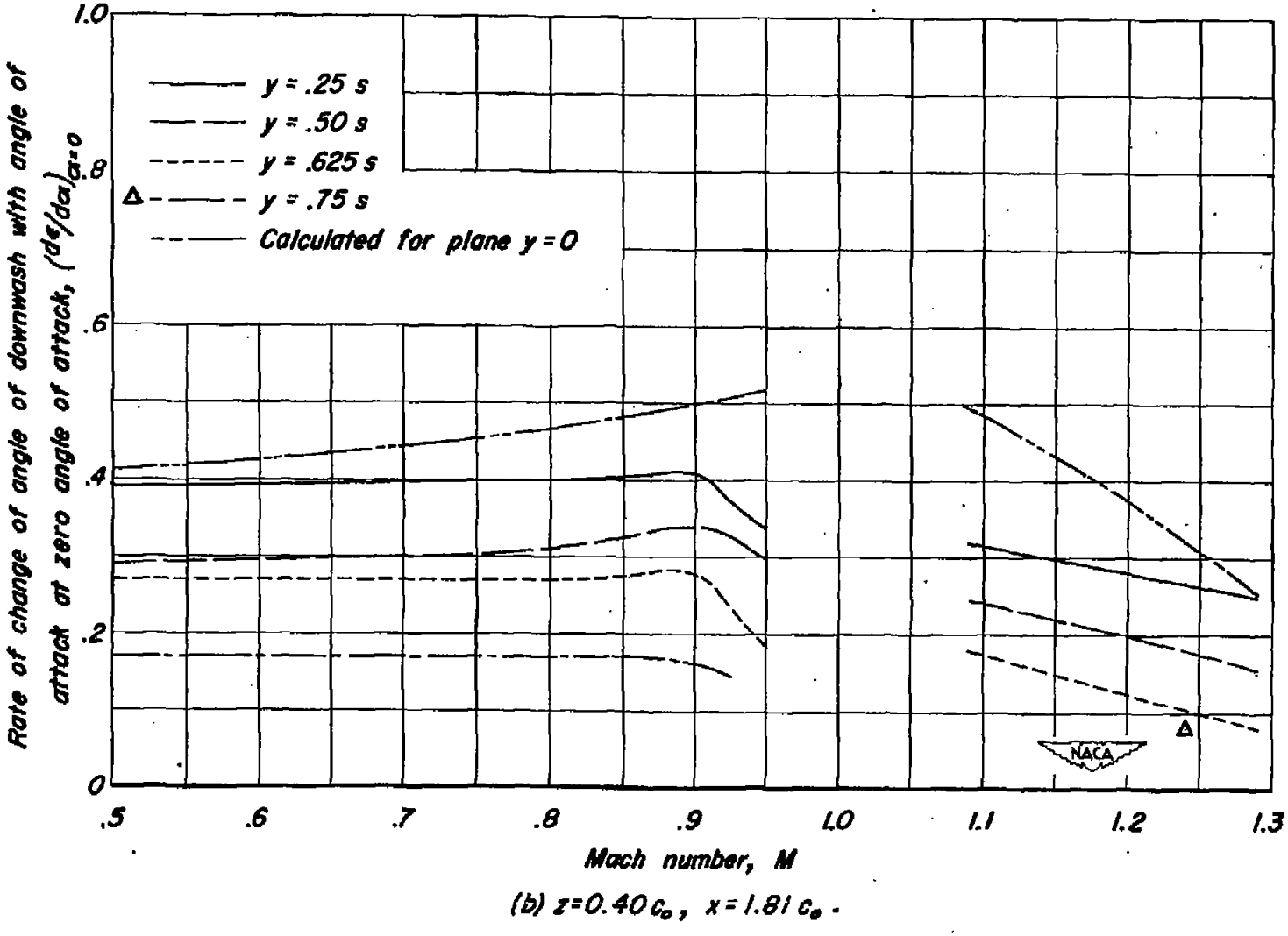

(b) $z = 0.40\,c_o$, $x = 1.81\,c_o$.

Figure 7. – Concluded.

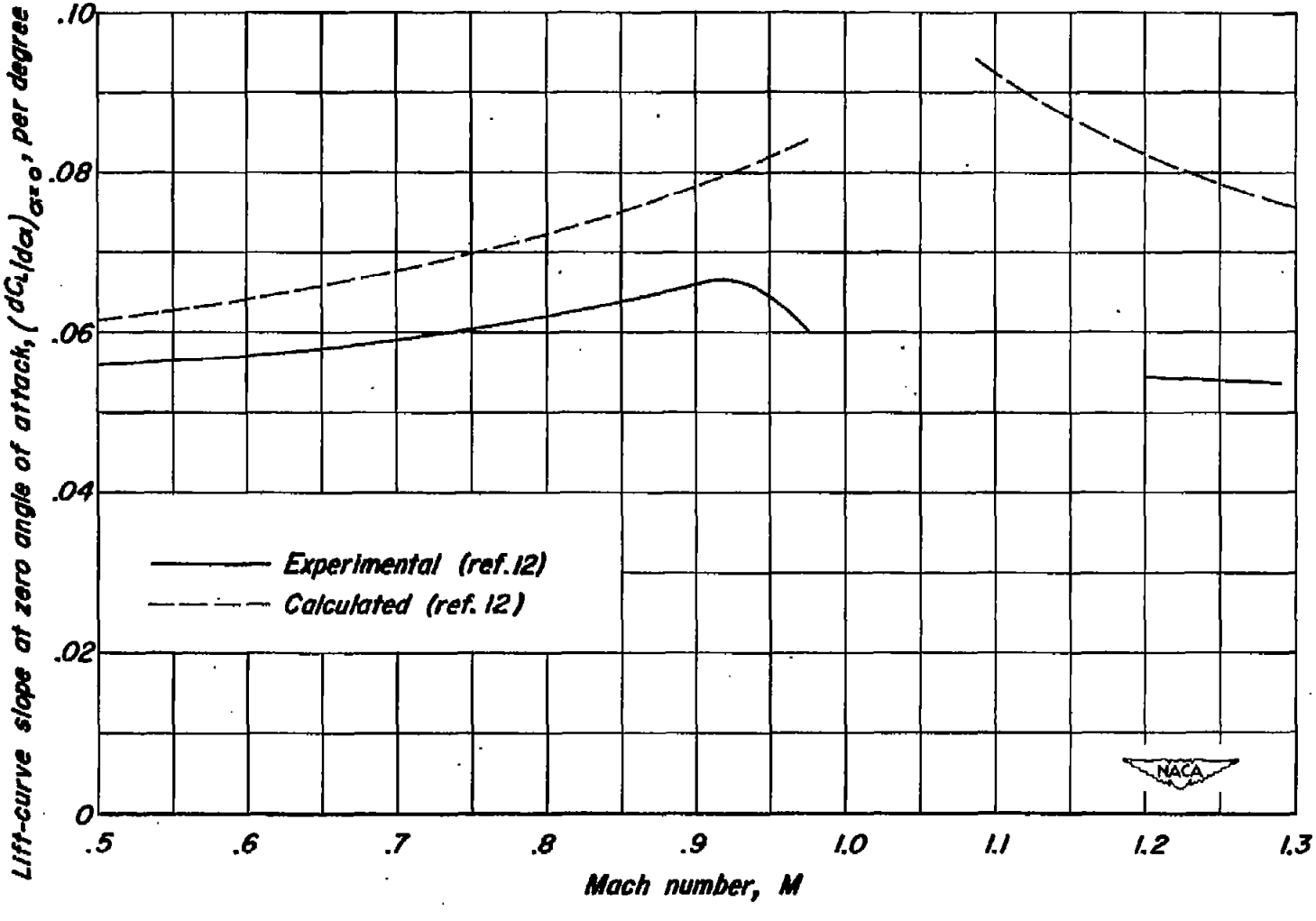

Figure 8.- Variation with Mach number of experimental and calculated lift-curve slopes at zero angle of attack.

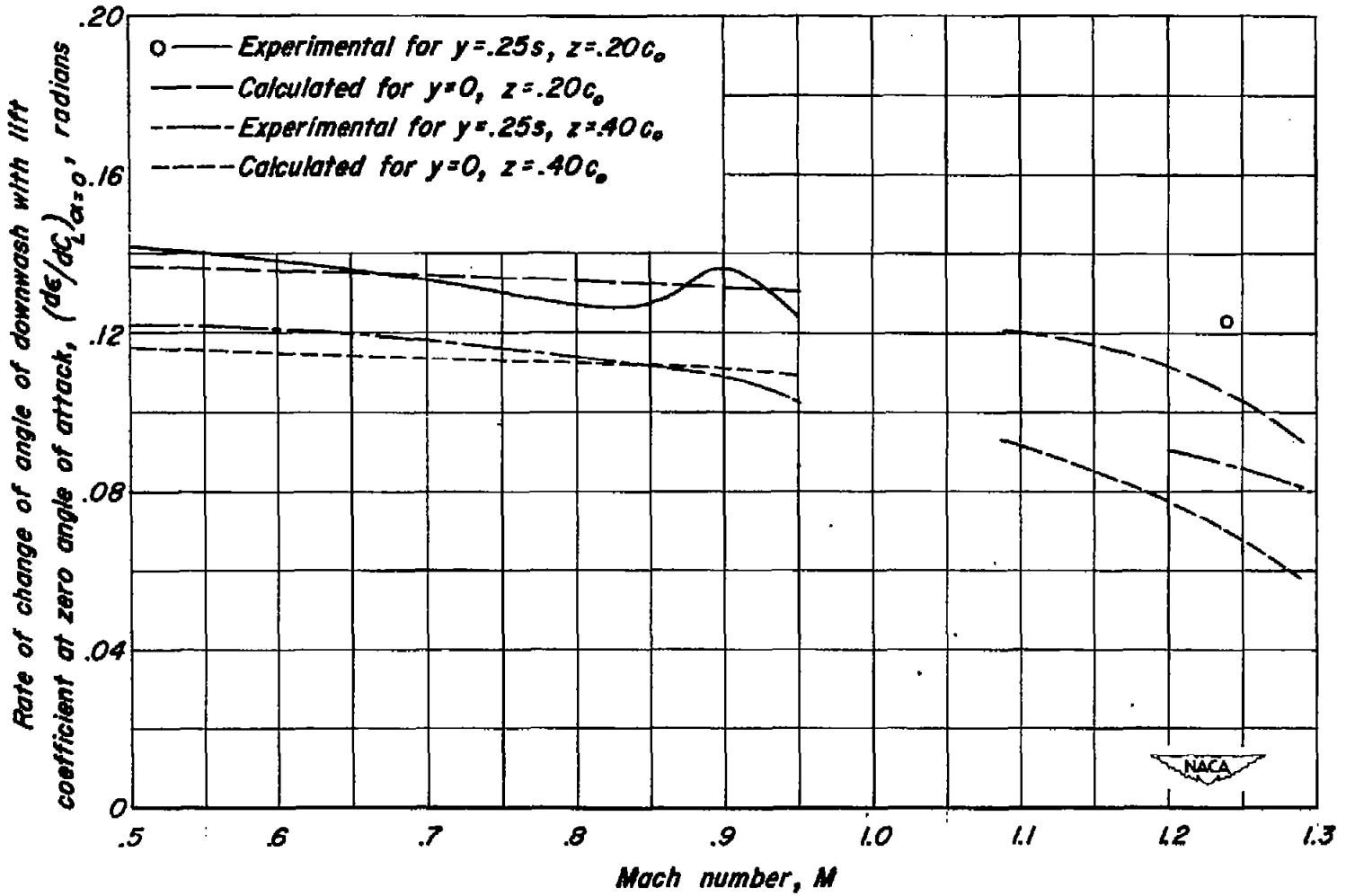

Figure 9. - Variation with Mach number of rate of change of angle of downwash with lift coefficient at zero angle of attack; z,0.20c_o and x,1.86c_o; z,0.40c_o and x,1.81c_o.

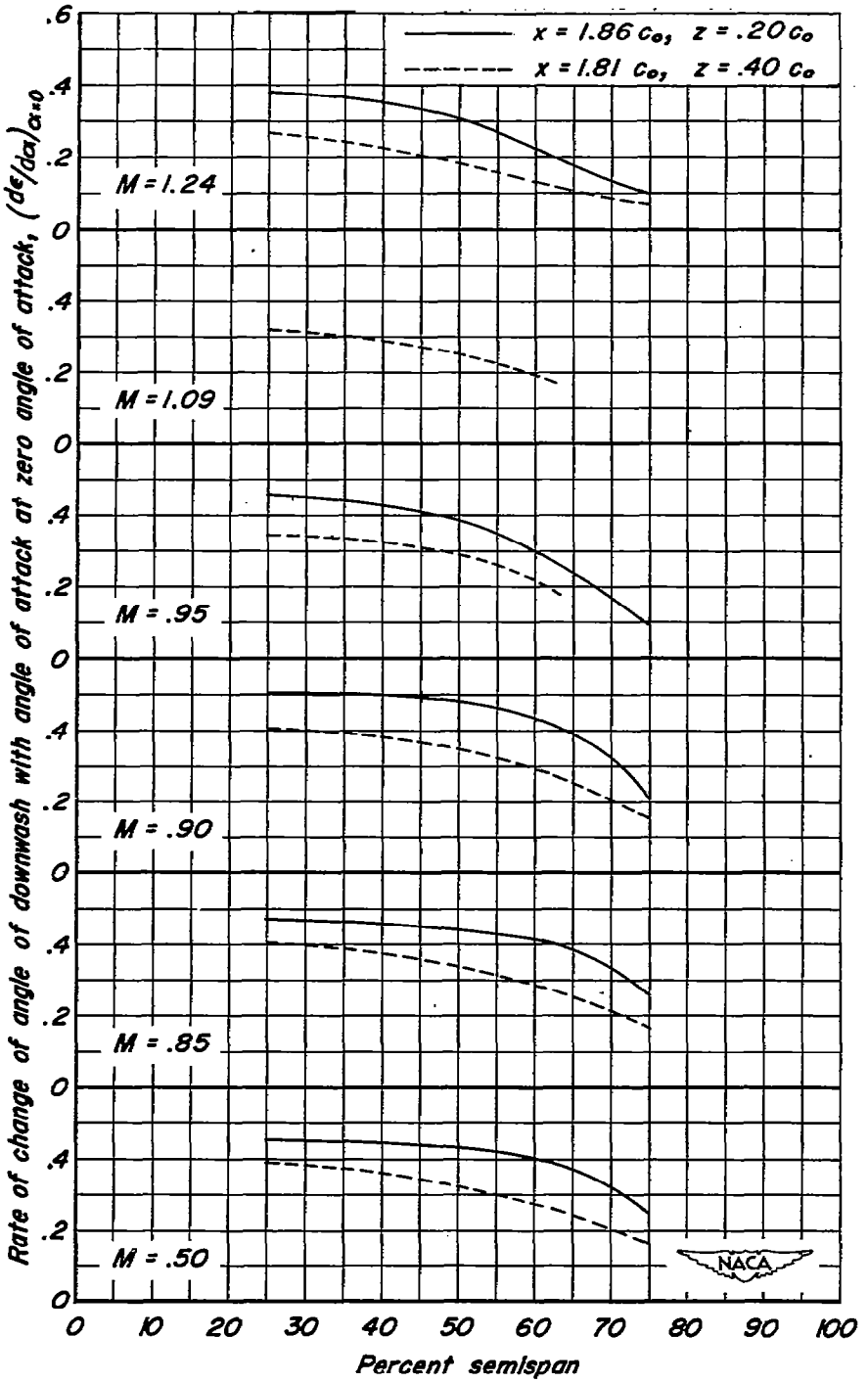

Figure 10.– Spanwise variation for several Mach numbers of rate of change of angle of downwash with angle of attack at zero angle of attack.

[redacted]

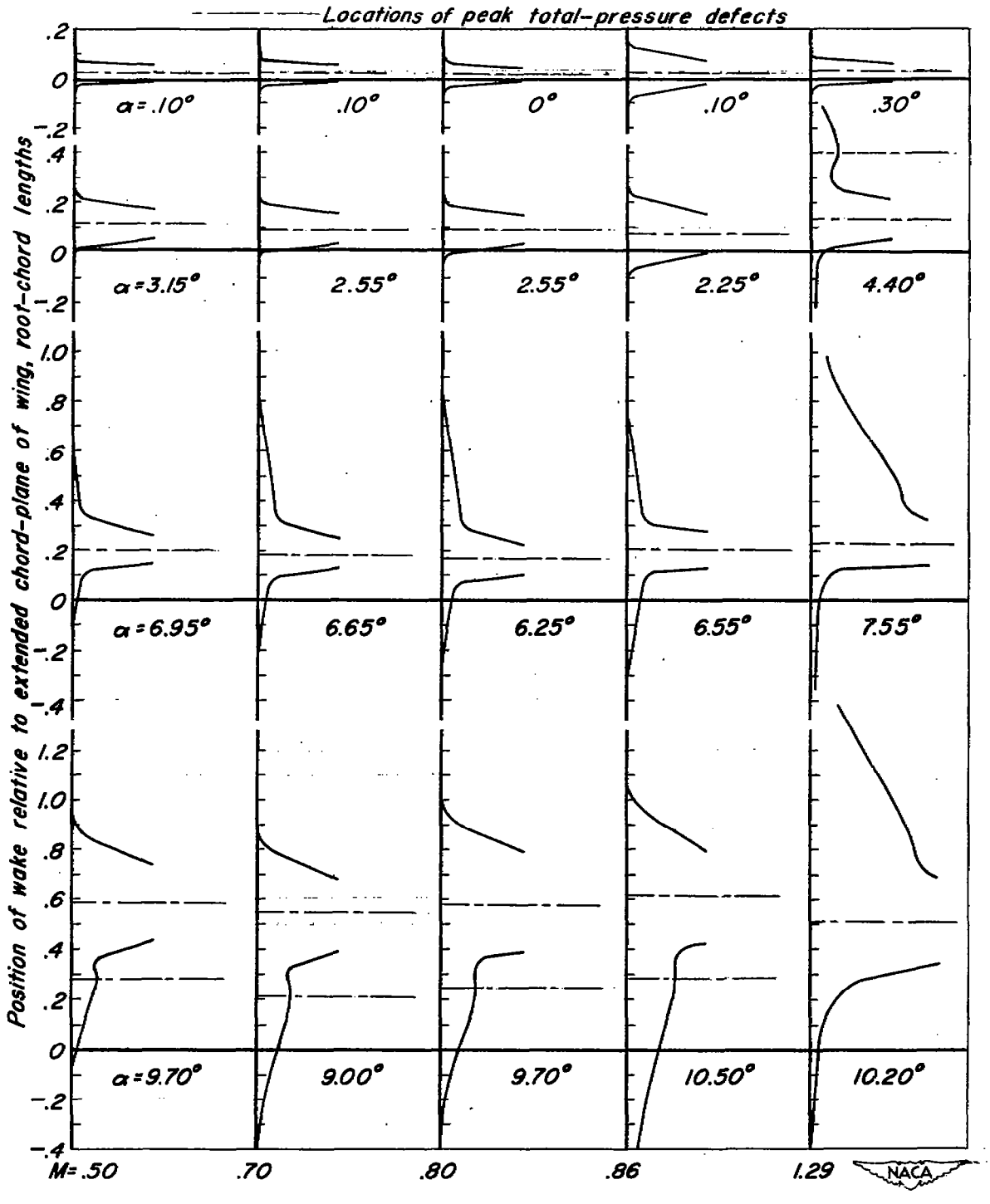

Figure 11.- Wake profiles measured at the 50-percent-semispan station 3.44 root-chord lengths downstream from the trailing edge of the wing.

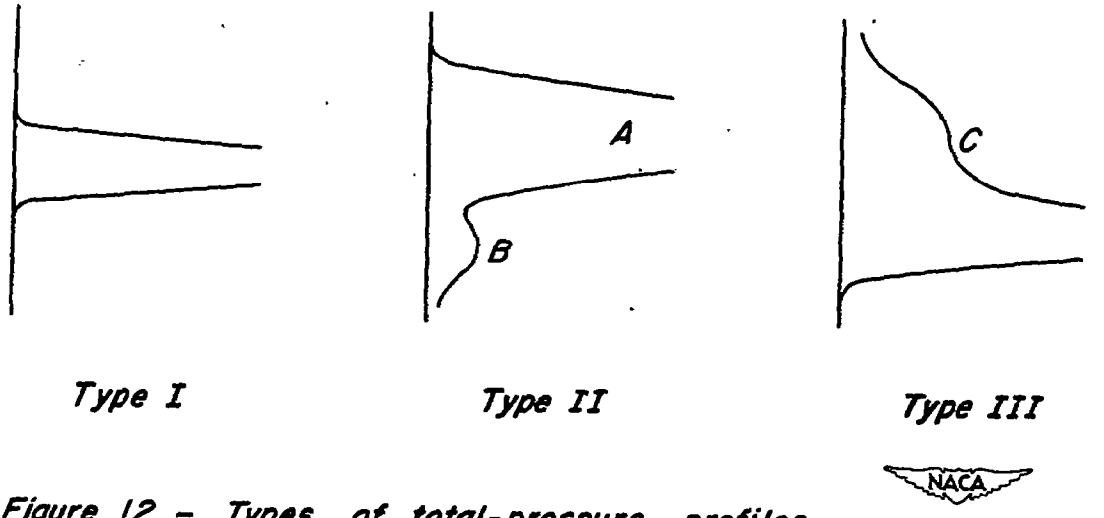

Figure 12. - Types of total-pressure profiles.

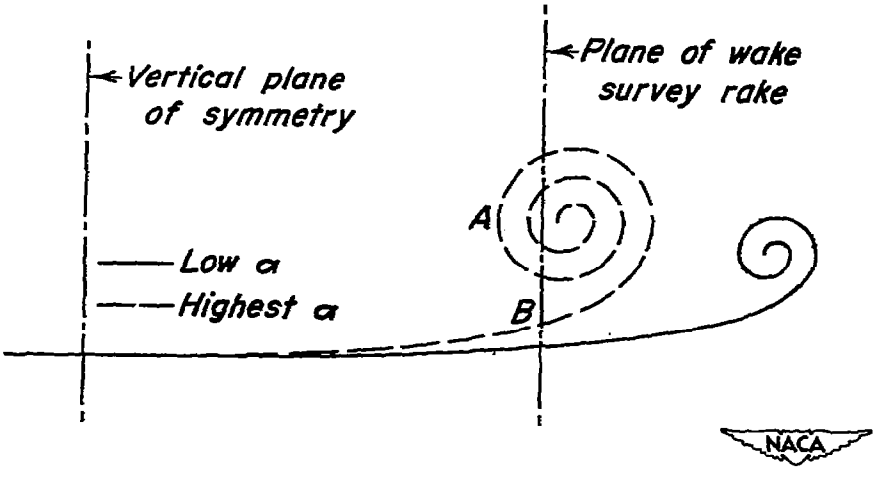

Figure 13. - Rolling up of trailing vortex sheet.

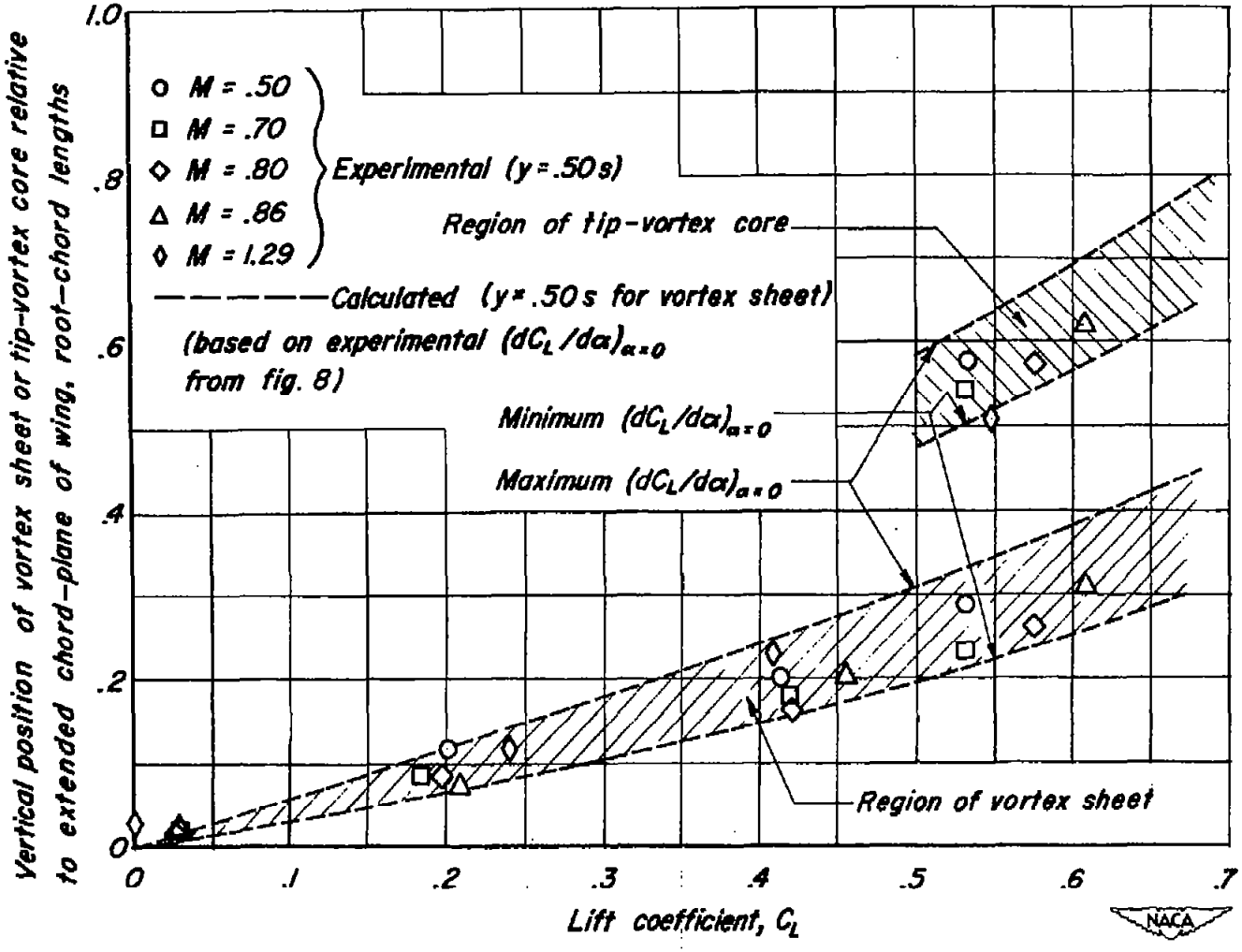

Figure 14.- Variation with lift coefficient of position of vortex sheet and of center of tip-vortex core relative to extended chord plane of wing at distance of 3.44 root-chord lengths downstream from trailing edge of wing.